MTHE393 Final Report

Shivam Sood Tristan Ellison Drew Colangelo
Oscar Brown Quinn Bazuk

April 10, 2023

Contents

1 Problem Introduction

1.1 General Problem

The goal of this project was to design a controller for a black box system and select an application for that controller. To begin this project the team began an ideation process to first select an application.

1.2 Application Selection Process

Several potential single input, single output (SISO) applications for the system were considered. Many of these systems were more complex than a SISO system and required several assumptions to be made. For this reason all possible inputs that would be required to completely solve the system would be held at the ideal constant rate with exception of the specified input-output pair to be considered.

1.2.1 Solar Panel Optimal Orientation

This application would be described by a system which would optimally orient solar panels relative to the suns position in the sky, such that they are capable of producing the most electricity. The input provided to the system would be the suns position in the sky which is determined using two angles, azimuth and zenith[1]. An assumption of the problem would be that this information could be compressed and delivered to the system as a single input. The output of the system would be the degree of rotation of the solar panel. A few more significant assumptions to solve the problem would be that the panels themselves are only allowed to rotate horizontally and not pivot vertically, or assume ideal vertical orientation, constant weather, and that the panels remain fixed in one location.

1.2.2 Nuclear Power Regulation

The second application would be investigating one of the control mechanisms employed by nuclear reactors to regulate their power production. Fuel rods within the reactor are comprised of a material which absorbs a portion of the neutrons released by radioactive isotopes when subjected to nuclear fission. The fuel rods are lowered directly into the reactor core where the level of insertion correlates to the degree of absorption[2]. Within this system the current power output of the reactor would be the input, and the output would be the corresponding height adjustment of the control rods to safely and optimally maintain power production. The assumptions made would include negligible decay of the control rods, constant amount of uranium within the reactor, operable temperatures, and no malfunction.

1.2.3 Missile Launcher Guidance

The third application considered was the technology used within missile guidance systems. Realistically this system is contingent on a multitude of factors

and would require imaginably a significant number of assumptions to deal with the amount of inputs and outputs required to guide a missile. An example of the assumptions made in this system would be a constant wind speed, designed for a single missile type, stationary target, target within range, and the rocket be capable of achieving necessary speeds. The simplified version of the problem would employ the single input of the global positioning coordinates to produce the output of the trajectory required by the missile launcher to accurately deliver the payload.

Though each of the three aforementioned applications were intriguing, the team had two final options that were considered to be best. Both of these applications are described below in greater detail.

1.2.4 Power Flow Controller

Of all the applications the team considered, designing a control system to regulate the flow of energy produced off-grid was one of the more promising ideas. This control system would be implemented on personal power generation systems, like solar panels. Most people with solar panels use the energy they create for personal applications. However, since solar panels are highly efficient, it is often the case that they produce more energy than required for their needs [3]. In these cases, extra power can be sent back to the grid at a guaranteed rate of $0.39 per kWh in Ontario [4]. This is a substantial amount of money, as a house with 40 standard solar panels can produce over 14,000 kWh of energy each year, earning approximately $5,500 per year if all the energy is sold [4].

This system would maximize the profits a solar panel owner receives by sending excess energy to the grid, while ensuring they still have enough power for their daily needs. In this control system, the input is the amount of power the solar panel system is generating. The output of the system is the amount of power to be kept for personal use. Both the input and output are measured in kWh. In this system, the output is combined with new inputs and then inputted again into the system. In other words, the power to be kept is combined with the new power generated, and then from there a new decision is made on how much energy to keep.

To implement this system, several assumptions need to be made. First, it is assumed that the technology to measure and direct the flow of energy exists. It is also assumed that this technology can record and update at a fast rate, for example every second. This is important because faster update times produce a higher level of accuracy. Another assumption on the system is that it is implemented somewhere such as Ontario, where you can sell energy to the grid.

The implementation of this control system has many stakeholders. A key stakeholder is the customer who would buy this control system for their solar panel system. This system positively influences this stakeholder because they can

earn money selling their excess power to the grid. Another stakeholder is the Ontario government, as they will be purchasing power from the users of the system. The manufacturer of the system is also a stakeholder because they have a new product to produce and sell. An additional stakeholder, and possibly the most important one, is society. Society benefits from the mass implementation of this system because it promotes clean energy, which is one of the best ways to mitigate climate change.

The Triple Bottom Line was considered when designing this system. As mentioned in the previous paragraph, society benefits from the implementation of the system as it reduces climate change. Since the system helps fight climate change, it obviously benefits the environment as well. Another way the system positively impacts the environment is it makes solar energy more accessible. A major problem that currently exists with solar power is the high cost. Nonetheless, with excess power being sent to the grid in exchange for money, solar panels become more affordable. If this system was implemented, it would be a profitable investment. It's most likely that sales will be high, as the cost of the product will likely be less than the amount of money the user could potentially earn selling power back to the grid.

While this system is beneficial to the environment, society and the economy, it is expensive to implement. The first step of implementation is to acquire the necessary technology. The next step is to add these control systems into existing solar panel systems. The solar panel systems will need to be altered to cooperate with this new technology. To estimate a total cost of implementation, this system was compared to a solar inverter, which is on a similar scale. With this information in mind, the estimated cost of each system is between $1000-$1500 [5]. If this system were to be implemented on a large scale, for example 1000 houses, the cost would be around $1,250,000.

1.2.5 Brainwave Measurement

Sleep quality and duration is a major factor in living a healthy life. Sleep has been proven to be a statistically significant contributor to decreasing all-cause mortality [6]. Not only does reduced sleep quality and duration contribute to physical illnesses, it also negatively contributes to memory and mental health [7][8].

As this was the selected application, please refer to Section 1.5 for an in-depth analysis on key stakeholders as well as Section 5 for a Triple Bottome Line analysis.

1.3 Evaluation of Potential Applications

To determine which application to move forward with, the team used a weighted evaluation matrix (WEM) to guide the decision process based on what was

thought to be the most important factors in choosing an application. The WEM used is shown below in Table 1 as well as a breakdown of how the score allocation was determined in Table 2.

		Power Flow Controller		Brainwave Frequency	
Criteria	Weight	Score	Weighted	Score	Weighted
Societal Impact	4	3	12	5	20
Environmental Impact	4	5	20	3	12
Economic Impact	4	3	12	4	16
Cost	2	1	2	2	4
Technical Feasibility	3	2	6	4	12
Innovation	3	3	9	5	15
Total (Sum)			**61**		**79**

Table 1: Weighted Evaluation Matrix

Based on the weighted evaluation matrix (WEM) the brainwave measurement controller was deemed to be the best idea. This idea stood out in two categories, technical feasibility and innovation, which propelled it to being the decided upon idea. For technical feasibility the team reasoned that as these devices have already been created and that our potential unit would be a standalone item, this would be easier to implement than a power flow controller. The power flow controller seemed more difficult to implement as connecting this to an existing power grid could create many complications not seen during a testing phase. In terms of innovation the brainwave measurement unit is cutting edge technology, only recently coming out, making it a more innovative idea, as well as the fact that it has potential to be applied to other control applications. Though the positive environmental impact of the power flow controller was significantly more pronounced, this category alone was not enough to provide the system with a high enough score to be chosen over the brainwave measurement system based on the team's scoring system.

		Score Description				
Criteria	Weight	1	2	3	4	5
Societal Impact	4	Strong negative impact on society	Moderate negative impact on society	No positive or negative impact on society	Moderate positive impact on society	Strong positive impact on society
Environmental Impact	4	Strong negative impact on environment	Moderate negative impact on environment	No positive or negative impact on environment	Moderate positive impact on environment	Strong positive impact on environment
Economic Impact	4	Significant negative effect on the economy	Moderate negative effect on the economy	No negative or positive benefit to the economy	Moderately benefits the economy	Significantly benefits the economy
Cost	2	Extremely expensive to implement	Expensive to implement	Slightly cost effective to implement	Cost effective to implement	Extremely cost effective to implement
Technical Feasibility	3	No current technology supports creation of this device without egregious assumptions	Minimal technology to support device creation and several assumptions required	Some supporting technology and moderate assumptions required	Vast amount of technology supports creation of device only moderate assumptions required	Vast amount of technology supports creation of device, minimal assumptions required
Innovation	3	Device performs worse than existing options	Minimal gain using this system	Control system offers potential gain compared to existing systems	Control system performs better than several existing options	Control system performs better than several existing options and can be applied to other systems

Table 2: Scoring Breakdown for WEM

1.4 Application Problem

Insomnia and poor sleep quality is a problem that one in three people experience [9]. Sleep quality is an important factor in an individual's life, in fact,

improving sleep quality has been proven to be a statistically significant contributor to decreasing all-cause mortality [6]. Not only does reduced sleep quality and duration contribute to physical illnesses, it also negatively contributes to memory and mental health [7] [8].

Typically, people with insomnia have two options for treatments, the first being cognitive behavioral therapy (CBT-I), and the second being prescription medications. CBT-I can assist a patient in managing or eradicating pessimistic thoughts and behaviors that hinder their ability to fall asleep and is often the initial course of action advised for individuals with insomnia. Generally, CBT-I proves to be as effective or more effective than sleep medications. Getting to sleep and staying asleep can be aided by prescription sleeping pills. Typically, doctors caution against use of these pills for a duration exceeding a few weeks, but there are several medications that have been authorized for extended usage [10].

Insomniacs are people who experience similar symptoms to those listed above. More specifically though, during sleep, insomniacs are said to exhibit increased alpha brainwave activity, whereas, the average human experiences delta or theta brainwave activity [11]. By creating a controller to impose a sleep-like state, the goal would be to control the subjects brain frequency using Transcranial Direct Current Stimulation (tDCS) in real time. TDCS is capable of both suppressing and invigorating neural activity in different regions of the brain [12]. TDCS works by sending minuscule electric currents into the brain to alter its frequency [13]. Creation of a device such as this provides potential treatment to a problem affecting one third of people around the world and could significantly increase their quality of life.

1.5 Stakeholders

There are many key stakeholders in this application, the first being the insomnia patients as they are the main beneficiary. Insomnia patients will experience improvements in their sleep quality, improving their learning and memory habits and overall physical and mental health [7] [8]. The next stakeholder in this application would be health insurance companies. This device would positively affect their bottom line and impact the rates they would provide to an individual. The Canadian government can also be considered a main stakeholder in this application as they would benefit from the reduced medical costs at hospitals and for prescriptions. Conversely, pharmaceutical companies would face the negative impacts from this application. The use of this device would reduce sleep related medication prescriptions and would significantly affect their profits.

1.6 Regulatory Standards

As discussed previously, tDCS involves the emission of a weak electrical current, traditionally via the placement of two electrodes attached to the scalp of a participant [14]. As the team plans to use this device to aid individuals with insomnia, it will be assumed that this is a medical device. The United States Food and Drug Administration (FDA) has three different classifications for medical devices, Class I, Class II, and Class III. As the class level increases, so does the seriousness of the device. For example, dental floss and band aids are Class I Medical Devices, while non-invasive blood pressure monitors are considered Class II [15]. Traditionally all non-invasive cutaneously administered (i.e., administered by the skin) electrical stimulation devices have been considered Class II. As such, the team will assume this is a Class II medical device to use the following guidelines:

- The 21 CFR Part 801 requirement defines labeling as a display of any "written, printed, or graphic matter upon the immediate container" of any Class II medical device. These labels must be legible and easily identifiable
- The 21 CFR Part 861 requirement states that Class II medical device manufacturers must demonstrate "reasonable assurance of the safety and effectiveness of the device."
- The 21 CFR Part 803 requirement mandates that all incidents involving Class II medical devices that have caused or contributed to a death or serious injury must be reported promptly. These records must be submitted within 10 days of the occurrence
- The 21 CFR Part 820 requirement outlines the unique methods, controls, and systems for "designing, purchasing, manufacturing, packaging, storing, and installing and servicing medical devices

These are the four key standards with which to keep in mind for any Class II medical device [16].

The National Library of Medicine conducted a study on the safety of tDCS and concluded that the four following parameters should be met when using these devices:

1. The current applied must be less than 2.5 mA
2. The current is applied through electrodes that are known to minimize skin burns at the specific current level being used
3. The current application duration is less than 20-60 min per session
4. Sessions are not more frequent than twice per day

This is not to say that exceeding these parameters will result in immediate or fatal consequences, however, at the time of the study and even today, the long

term use and effects of tDCS are still not well known enough to provide more specified advice [15].

Despite the regulations noted above, the reality is that due to gaps in research as well as unknown issues with tDCS, there are minimal standards in place outside of an experimental setting [17]. Due to this, several years of research are still required before better specified standards can be developed, thus it is assumed that the criterion noted above are sufficient for ensuring the safety of patients using these devices.

2 System Definition

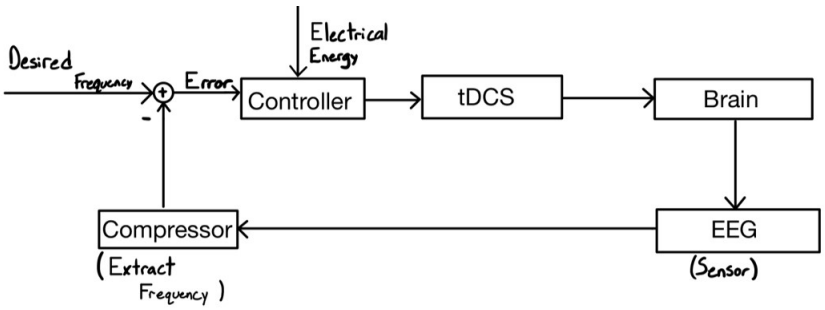

Figure 1: I/O Diagram of the System

Using the abilities of tDCS, the controller will take in the current state of a subjects brain using an electroencephalogram (EEG) as an input, record it, then apply the tDCS currents in an attempt to modulate the brainwave to meet the idealized waves for sleep. For the purpose of this application, we will consider delta brainwaves to be the most ideal. Delta waves occur when a person is in deep sleep, more technically known as non-rapid eye movement sleep. As this kind of brainwave appears to be the most sinusoidal the team reasoned that this would be the most attainable wave to model our idealized state after [18].

Figure 1 above shows a basic input output block diagram of the system. Here it can be seen that by using the error between the idealized brainwave frequency and current brainwave frequency as an input to the controller, the controller can activate the tDCS unit to apply the necessary amount of current required to change the patient's brainwave frequency to the idealized point. The brain is then once again measured using the EEG and the compressor is used to extract the brain's new current frequency and then fed back into the system to see if there is still error present and further action is required.

2.1 System Assumptions

The team has made two critical assumptions with regards to this control system:

1. The tDCS apparatus with the control system will be such that it does not cause discomfort or impact a patient's sleep negatively in any way
2. If the device accurately modulates brainwaves, the patient will actually experience a sleep like state

3 Black Box System Assumptions

The team will assume that the dynamics of the black box assigned to the team are representative of the dynamics of the selected application. Therefore the team is operating under the assumption that the behavior and performance of the black box accurately reflects those of the application it is intended to represent. This assumption is based on the premise that the black box has been properly designed and tested to accurately emulate the relevant aspects of the application's behavior. By making this assumption, the black box can be used to model and analyze the behavior of the application in a controlled and predictable manner. It is also assumed that the provided system targets, outlined in 4.5, are sufficient for verifying that the derived transfer function is accurate.

4 Technical Analysis

4.1 Linear Time-Invariant Analysis

For a system to be considered linear time-invariant (LTI) the following properties must hold:

1. Linearity requires two conditions to be true:
   (a) **Homogeneity**: Let $a \in R$. The system output to the input, au(t), is ay(t)
   (b) **Superposition**: Let $\tilde{y}$(t) be the output of the same system subjected to $\tilde{u}$(t) as an input. When this system is subject to u(t) + $\tilde{u}$(t) as the input, the output must be y(t) + $\tilde{y}$(t)
2. **Time-Invariant** If the input is shifted by T seconds (i.e., u(t-T)), then the output must also be shifted by the same amount of time (i.e, y(t-T))

To test for homogeneity the team needed to determine if providing a scaled input, say u(t) = 5*sin(t), would be equivalent to scaling the output, i.e., 5*y(t) when u(t) = sin(t). As seen in Figure 2 below, the functions with a scaled input and scaled output have been graphed together and are match up in a

nearly identical manner. This allowed the team to conclude the system was homogeneous.

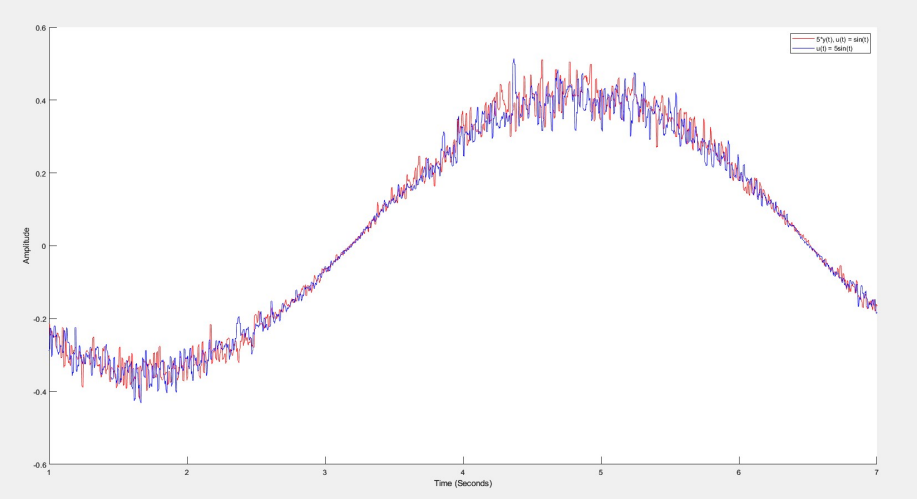

Figure 2: Homogeneity of the system

Next the team looked to confirm that the system had the property of superposition. To do this an input of t + sin(t) was used and its output was graphed, while the output data of an input u(t) = sin(t) and $\tilde{u}(t) = t$ was added together and graphed. When each of the graphed functions were plotted, as shown in Figure 3, it was clear that superposition must be a property of this system as the output graphs were almost identical.

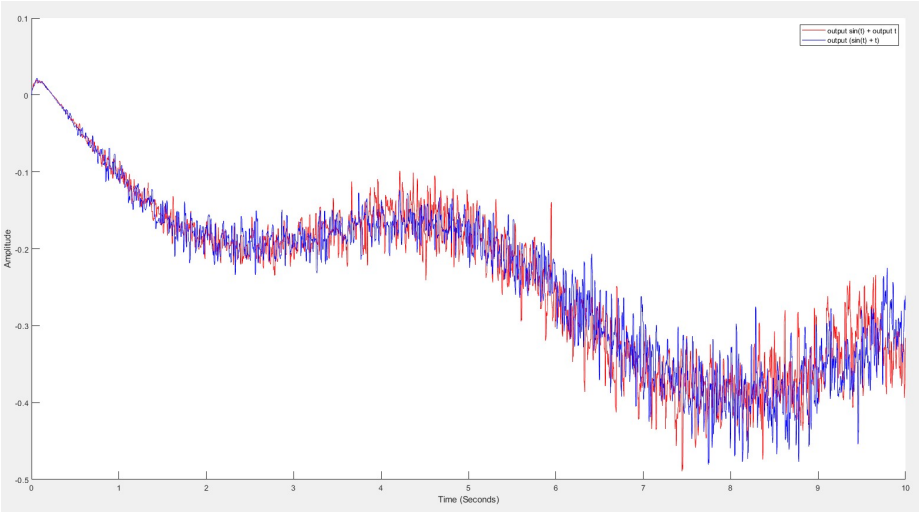

Figure 3: Superposition property of the system

Finally testing if the system was time-invariant, the team decided to use sin(t-π) as the shifted input function. Then applying the shift to y(t), i.e., y(t-π) when u(t) = sin(t). Each of the shifted functions was plotted, as shown in Figure 4 below, and based on the generated graphs it is clear that a shift in the input is equivalent to a shift in the output. Hence the the system is time-invariant. Therefore, as this system was found to be both linear and time-invariant, it is an LTI system. Now that this has been verified the team is able to justify the creation of Bode plots shown in Section 4.3 and from those plots, the derivation of a transfer function described in Section 4.4.

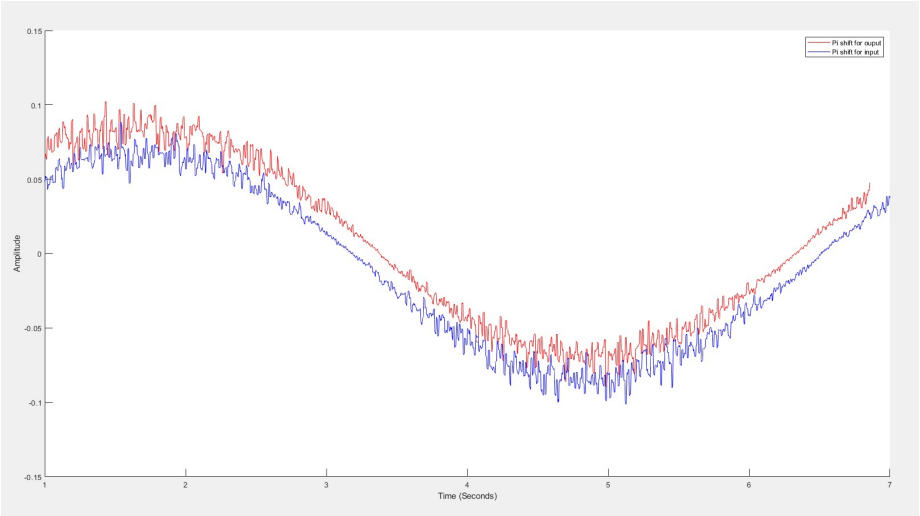

Figure 4: Time-invariant nature of system

4.2 Denoising

While inputting different graphs into the black box system, the team realized that the output data was too noisy to find phase shift and magnitude computationally. The noise would often create many zeroes within a close proximity, making it nearly impossible to examine properties like the output's period. Figure 5 is one example of a noisy output.

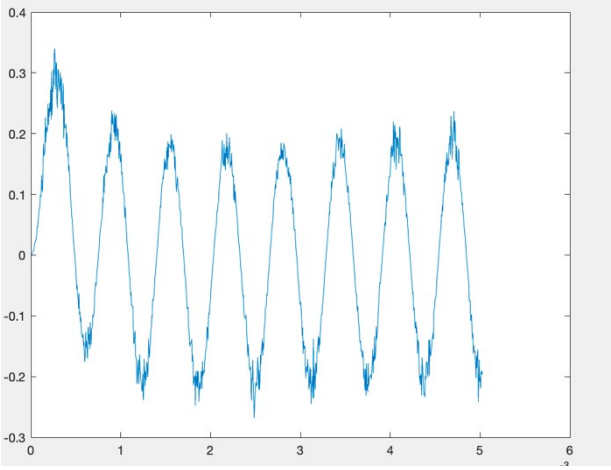

Figure 5: Raw output data from black box system

The first MATLAB function introduced was the 'smooth' function. However, the

team realized that when trying to calculate the magnitude of the graphs, there was still residual noise at the peaks and troughs. Under further investigation, the team learned that the 'smooth' function has a default rolling window of 5. In combination with the fast-sampling rate, this left the output with noise still inside.

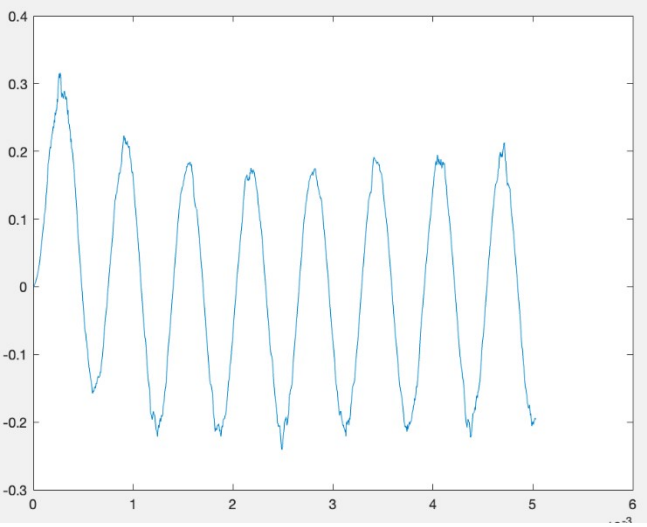

Figure 6: Output after 'smooth' function applied

The next function used was MATLAB's 'smoothdata' function. Smoothdata heuristically determines the optimal rolling window length and then outputs the noiseless signal. The team found the output to be easy to work with and analyze.

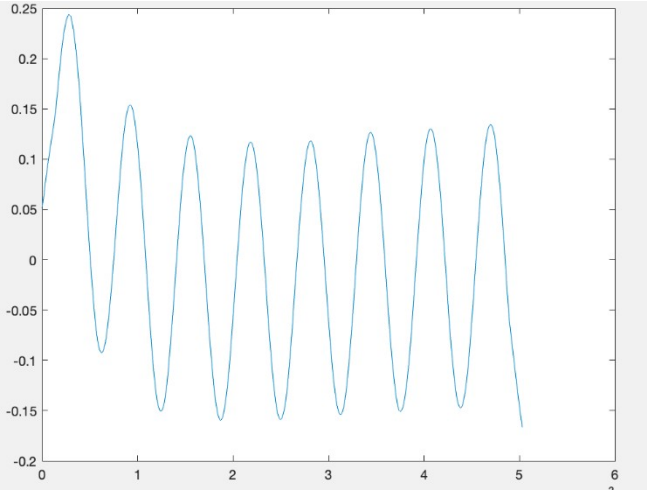

Figure 7: Output after 'smoothdata' function applied

4.3 Bode Plot Analysis

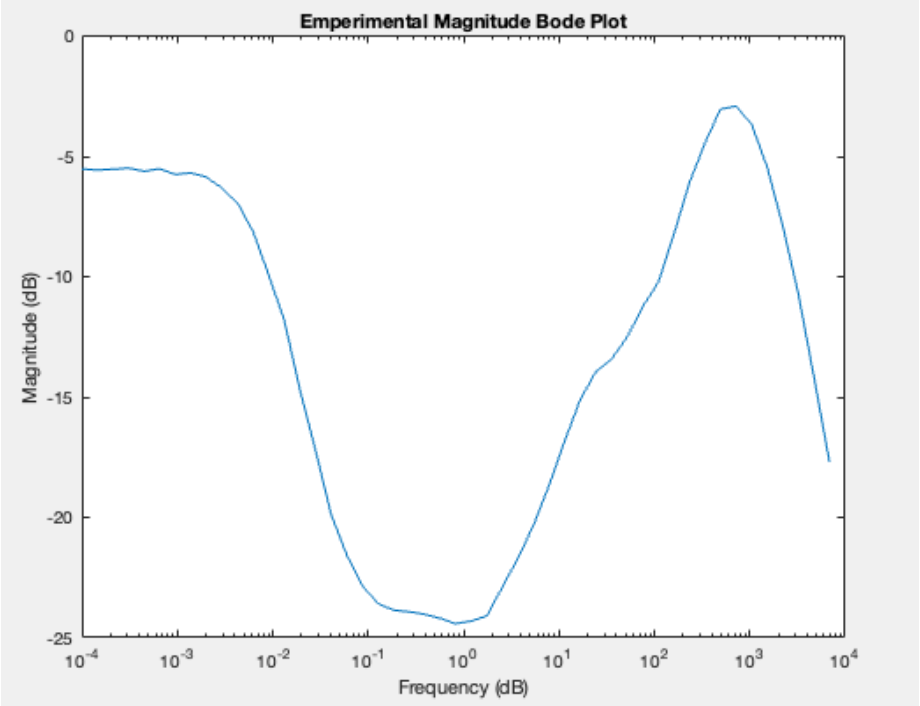

Figure 8: Amplitude versus frequency Bode plot

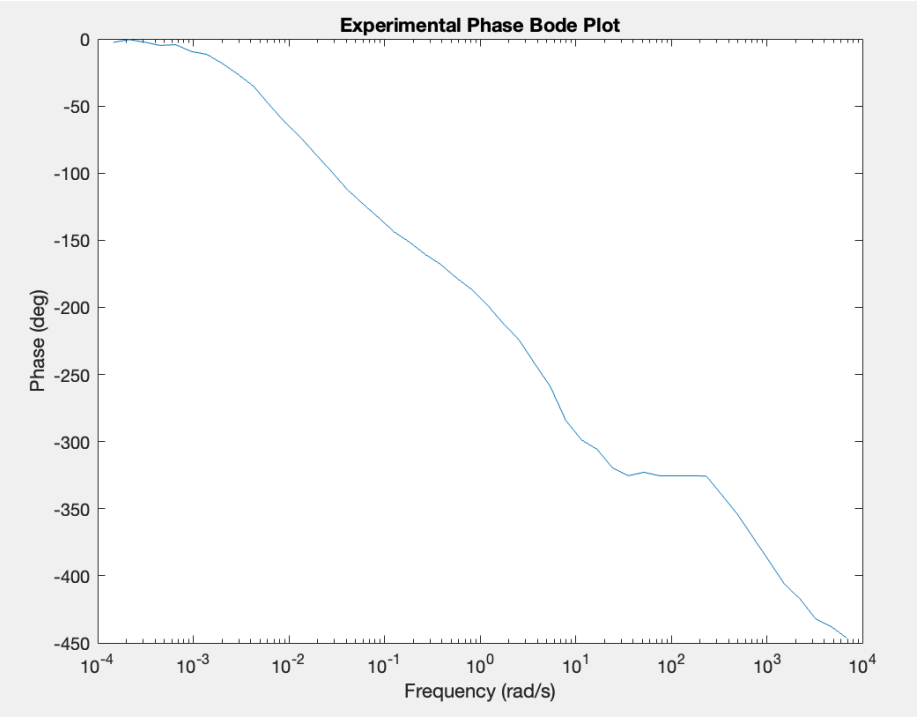

Figure 9: Phase shift versus frequency Bode plot

It is much easier to design a controller for a black box system when you understand the characteristics of the black box. One way of determining these characteristics is by creating bode plots and deriving a transfer function from these bode plots. Having a transfer function helps depict particular characteristics of the system like stable/unstable poles and stable/unstable zeros.

To compute the Bode plots, 50 logarithmically spaced data points in the interval $[10^{-4}, 10^{4}]$ were generated and each provided as a frequency ω for a sine wave $\sin(\omega t)$, which together were supplied as inputs for the system. While the refine output value for each independent trial remained the same, the step size value and end time varied according to the expression $stepSize = \frac{0.05}{\omega}$ and $endTime = \frac{16*pi}{\omega}$ respectively. The variation of step size was to accommodate for lower input frequencies requiring larger step sizes, while higher input frequencies required smaller step sizes. In effect, the step size for each successive trial grew proportionally to the input frequency. The signal output for each individual frequency was saved then plotted and smoothed to reduce noise interference.

The phase shift was then derived for each output plot by finding the first instance where the graph of the sine wave switched its sign from negative to positive after five periods. This was achieved by finding the first rising zero

after five periods. This approach allowed for the graph to reach a steady-state, ensuring that the phase shift was accurate.

The amplitude ratio was approximated by computing the maximum data point after five periods by y-value, for each unique trial. Although another possible approach would have been to take the average of all local maximums from each crest of the sine wave, after smoothing the plotted data, steady-state peaks were found to be within an acceptable range of one another. This was accomplished by creating a function in MATLAB to perform the above procedures, which was then called for each of the 50 initial frequency trials' data sets.

Two arrays were created to hold the phase shift and amplitude ratio for each trial, then plotted against a logarithmically spaced scale from the initial set of logarithmically spaced data points used for frequency inputs. This completed the team's Bode plot generation with Figure 9 and Figure 8 depicting the rate of change of the phase shift and amplitude relative to logarithmic change in frequency respectively.

4.4 Transfer Function Derivation

The transfer function was derived from the magnitude plot. The magnitude of each zero and pole can be found by a significant change in the magnitude bode plot. When the magnitude plot encounters a pole, the magnitude's slope decreases at 20 $\frac{dB}{decade}$, conversely, when a zero is encountered the slope increases at 20 $\frac{dB}{decade}$. Figure 11 labels poles with x's and zeros with o's.

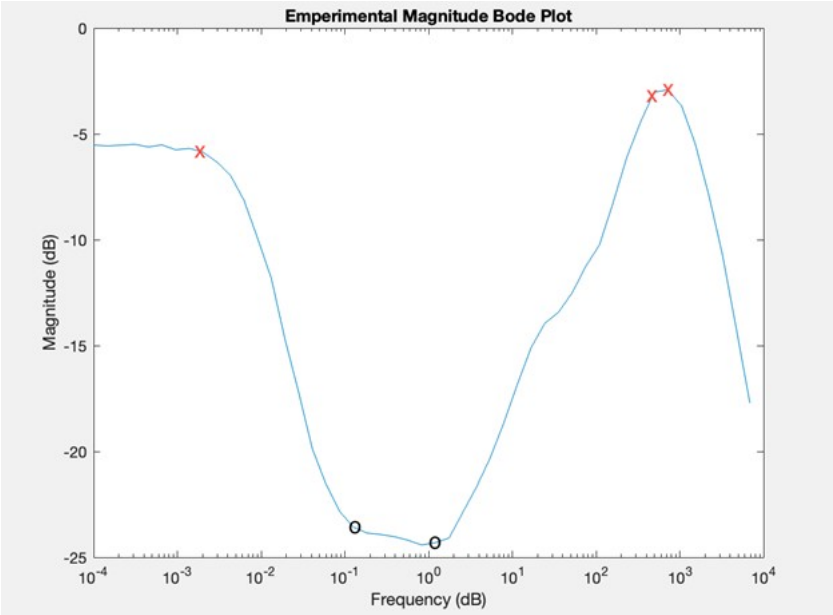

Figure 10: Poles and Zeros of Magnitude Plot

Since the system is BIBO, all the poles are in the left-half plane (LHP). The zeros' exact locations, however, could be in right-half plane (RHP) or LHP. The team tried all combinations of zeros in the RHP and LHP, and as there are only two zeros, there are four possible transfer functions for this magnitude plot.

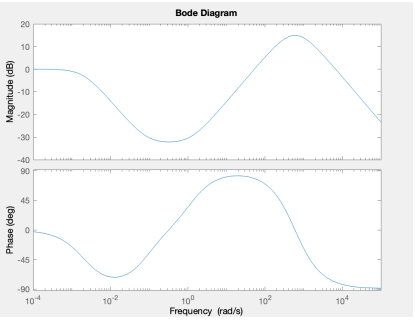

(a) Numerator = $(\frac{s}{0.087}+1)(\frac{s}{1.21}+1)$

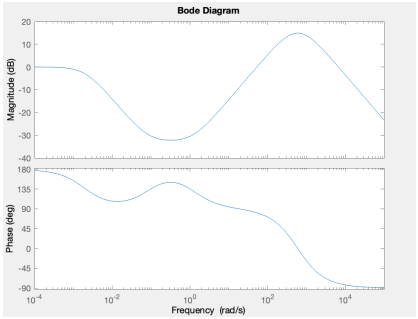

(b) Numerator = $(\frac{s}{0.087}+1)(\frac{s}{1.21}-1)$

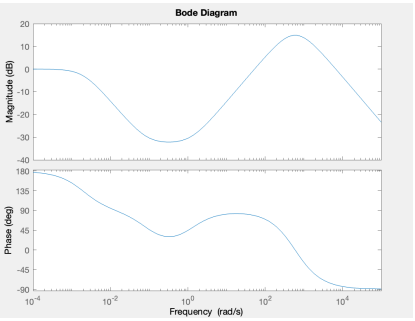

(c) Numerator = $(\frac{s}{0.087}-1)(\frac{s}{1.21}+1)$

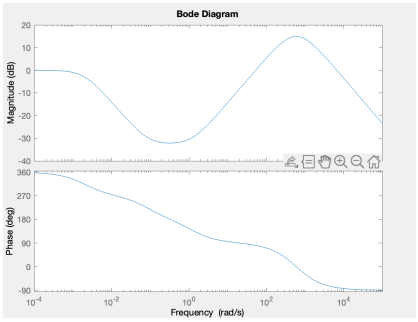

(d) Numerator = $(\frac{s}{0.087}-1)(\frac{s}{1.21}-1)$

Figure 11: All possible combinations of RHP/LHP zeros to find the transfer function

When compared to the experimental phase shift plot, it's clear that the final bode matches the Blackbox system. Thus, the transfer function is then

$$P(s) = \frac{(\frac{s}{0.087}-1)(\frac{s}{1.21}-1)}{(\frac{s}{0.002}+1)(\frac{s}{494.2}+1)(\frac{s}{719.7}+1)} \tag{1}$$

4.5 Controller Design

Once a satisfactory transfer function had been derived from the experimental Bode Plot by the process described in Section 4.3, the design process of the control system began.

The control system design process entailed first producing a Proportional Integral Derivative controller of the derived transfer function model and adjusting the parameters K_p, K_i, K_d and τ_f, to produce a stable output according to the provided performance specifications for a stepped input. Once the desired output was achieved for the corresponding tuning parameters, the next step included substituting the derived transfer function model for the block box itself,

then subjecting it to a PID controller with the objective again to attain a stable output within the performance requirements for a stepped input. The provided requirements are outlined in the table below.

Step Response Parameter	Target Value
Steady State Error	± 0.08
Rise Time (s)	9
Overshoot	0.2
Settling Time (s)	15
Settling Time (ϵ)	0.08

4.6 Implementation of Controller on Transfer Function Model

Once the PID controller, including a low pass filter, had been assembled in MATLAB using Simulink, the derived transfer function was expanded.

$$p(s) = \frac{9.49938s^2 - 12.32069s + 1}{0.00140s^3 + 1.70647s^2 + 500.00341s + 1} \tag{2}$$

The coefficients of polynomials in the numerator and denominator of the expanded version of the derived transfer function were then inserted into the parameters of the transfer function block in the controller.

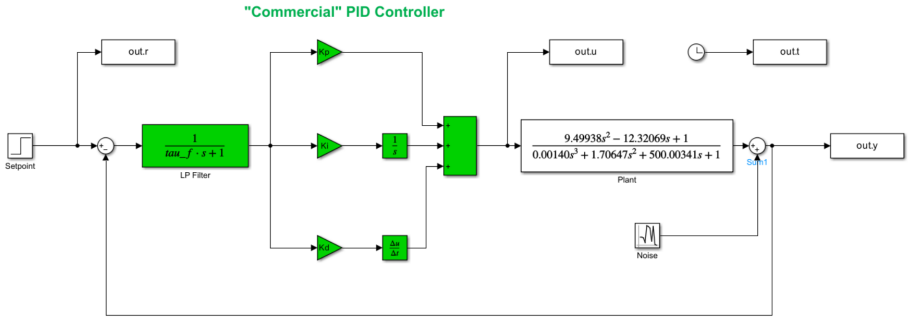

Figure 12: PID controller for transfer function model

Beginning at 0, values of K_p were adjusted increasingly in increments of 0.1 between the values 0 and 1. For the range of 1 to 30, K_p was increased in increments of 1. Values of K_p greater than 30 were not methodically tested since those values caused the steady state offset to increase and the output would converge to values slightly greater than 1. For each new incremental increase in K_p, the value of K_i was adjusted increasingly in increments of 0.1 between the values 0 and 1, and in increments of 0.5 for values greater than 1, until 10. Any value of K_i greater than 10 was not methodically tested as for those values the overshoot in the output would strictly increase and far exceed the target

specifications. For each new increment in K_i, the value of K_d was increased in increments of 0.1 between the values 0 and 2. Values of K_d greater than 2 were not methodically tested since those values would cause the output to diverge in some instances and were not practical to include. The value for τ_f fluctuated between 1 and 10 for all trials and was not tested according to any rules.

If at any combination of parameter values the output appeared to be stable and behave like the controller specifications, smaller adjustments were made to each parameter to check whether the output could satisfy the specifications. Each individual trial was conducted using the week 10 MATLAB script provided for tuning the PID controller.

Despite the rigorous testing method, no combination of parameters was found that would produce a correct output. Over the testing process, the transfer function model revealed to be a non-minimum phase system with two right hand plane zeroes. This caused any output of the controller that was stable, and almost satisfied all the specifications, to have severe undershoot beginning at the start of the step. This was sometimes preceded by an immediate impulse until 1. The other common case was a resultant output that would remain stable for relatively larger amounts of time, then suddenly experience undershoot before diverging in the opposite direction.

It was concluded that tuning the controller according to the black box should instead be investigated and prioritized if it would be more realistic to find a combination of parameters that produced a valid output, as after all, tuning the controller according to the transfer function served mostly as an approximation for the tuning of the black box controller.

4.7 Implementation of Controller on Black Box

Upon substituting the transfer function for the black box, we were unable to test the accuracy of the PID controller parameters found from tuning the controller according to the transfer function model. This was due to that fact that no combination of parameters for which the output of the controller of the transfer function model for a stepped input, was in the range of the performance specifications. Similar issues were encountered with the controller now configured with the black box, as were found when testing the controller.

After comparing the bode plot of the black box to the bode plot of the transfer function model, both behave like a non-minimum phase system, with two RHP zeroes.

After researching controller tuning methods, one possible solution required the state space be modified to include a parallel feedforward loop, consisting of a gain block connected to a transfer function block which held the function with 1 in the numerator, and s minus the value of the first right hand plane zero.

$$F(s) = \frac{1}{s - 0.087} \tag{3}$$

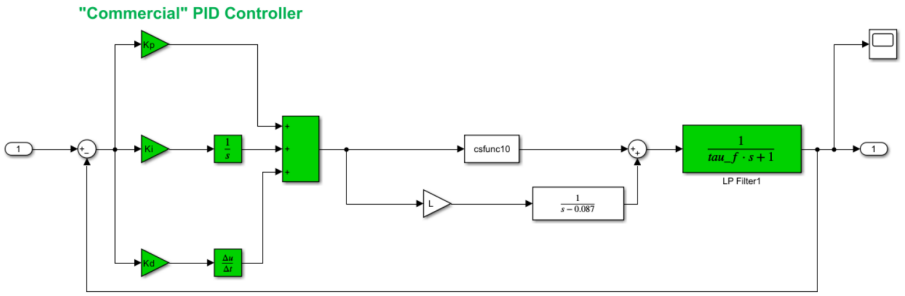

Figure 13: PID controller for black box

The value in the gain block was then varied until the system achieved minimum phase, consequently removing the instability about our right-hand plane zeroes. The values for K_p, K_i, and K_d, were initially approximated using the Ziegler-Nichols (Z-N) method. First the ultimate gain, K_u, and ultimate period, T_u, of the black box controller were calculated through finding the point where the system starts to oscillate, and the time required to complete one full oscillation when the system was at a steady state, respectively. More explicitly, the ultimate gain was calculated by applying a 180 degree phase shift on the bode plot of the black box from the starting value. Ultimate period is equivalent to one over the ultimate gain.

$$K_u = 0.321 * 0.1592 = 0.0511032 \tag{4}$$

$$T_u = \frac{1}{K_u} = 19.5682462 \tag{5}$$

The values for K_p, K_i and K_d were then calculated through using the corresponding set of relation between the tuning parameters, and the ultimate gain and period, for a PID controller with a filter, detailed in the Z-N method [19].

$$K_p = 0.6 * K_u = 0.6 * 0.0511032 = 0.03066 \tag{6}$$

$$K_i = 1.2 * \frac{K_u}{T_u} = 1.2 * \frac{0.0511032}{19.5682462} = 0.003134 \tag{7}$$

$$K_d = 0.075 * \frac{K_u}{T_u} = 0.075 * \frac{0.0511032}{19.5682462} = 0.0001959 \tag{8}$$

These values were used as a starting point for the controller tuning and were adjusted methodically, changing K_p first, then K_i, then K_d, and finally τ_f. The

values of the tuning parameters were adjusted through changing the coefficients of K_u, and T_u in their respective relations of the Z-N method.

$$K_p = 188.4422 * K_u = 188.4422 * 0.0511032 = 9.63 \tag{9}$$

$$K_i = 157824297.4 * \frac{K_u}{T_u} = 157824297.4 * \frac{0.0511032}{19.5682462} = 0.0412164 \tag{10}$$

$$K_d = 5743743900 * \frac{K_u}{T_u} = 5743743900 * \frac{0.0511032}{19.5682462} = 1.5 \tag{11}$$

Finally, acceptable outputs that satisfied the performance specifications were gradually being approached, and a combination of parameters, $K_p = 9.63$, $K_i = 0.0412164$, $K_d = 1.5$, $\tau_f = 10$, and a gain constant of $L = 100$, were found to produce a response to a stepped input well within the performance specifications. The figure below was generated by running the black box GUI to execute the modified state space containing the PID controller with a low-pass filter, for the black box, with a parallel feedforward loop.

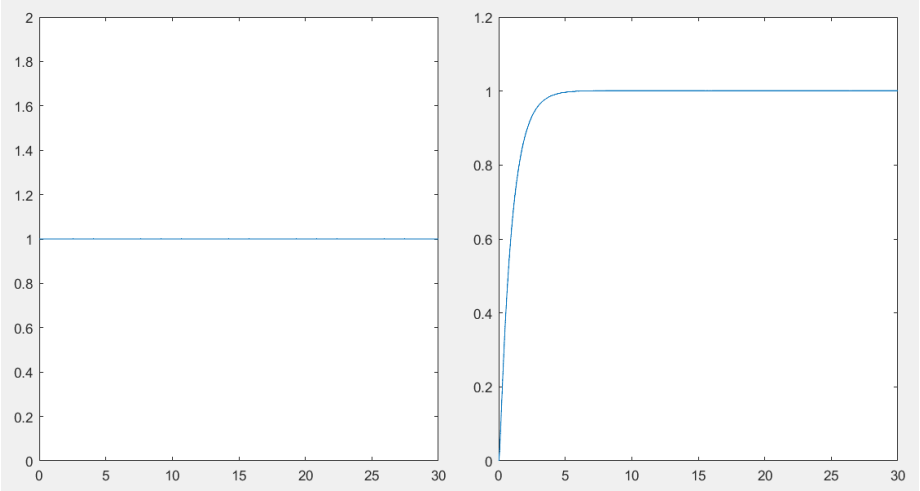

Figure 14: Output of PID controller for black box provided stepped input, $K_p = 9.63$, $K_i = 0.0412164$, $K_d = 1.5$, $\tau_f = 10$, $L = 100$

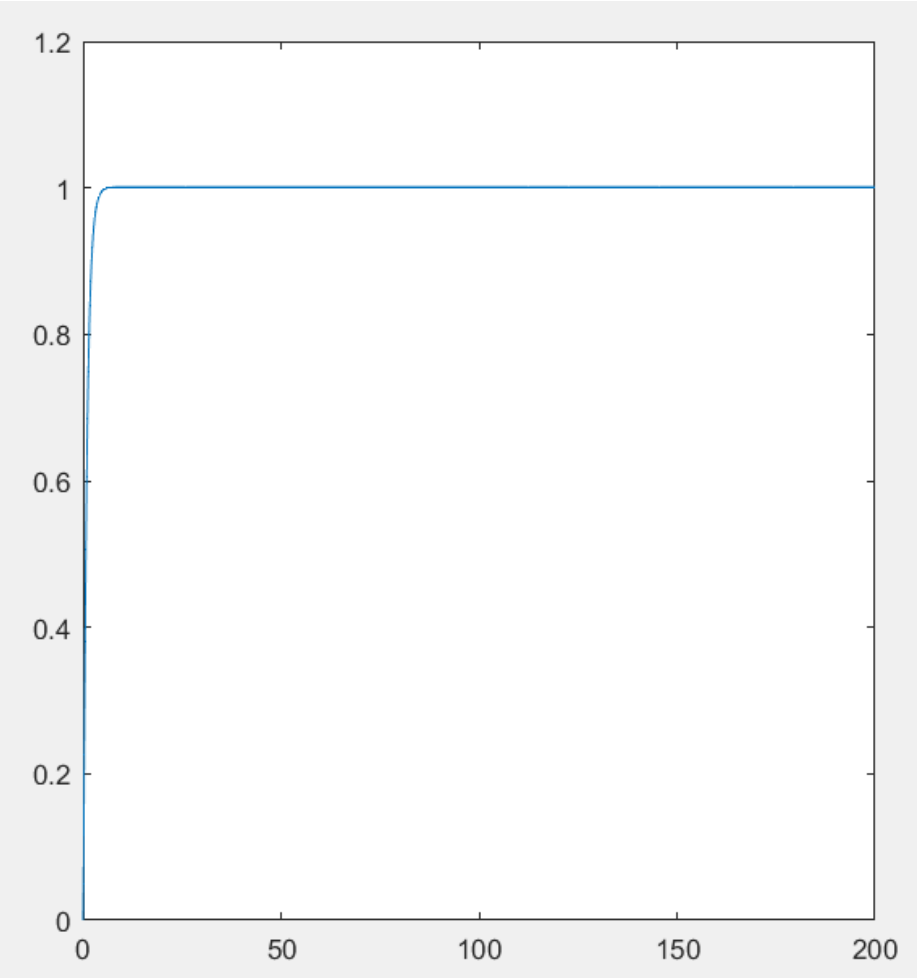

Figure 15: Output of PID controller for black box provided stepped input, $K_p = 9.63$, $K_i = 0.0412164$, $K_d = 1.5$, $\tau_f = 10$, $L = 100$, with 200 second runtime to show stability

An important note is that during the testing process the noise block in the state space was removed to tune the controller and determine which direction of adjustment to the tuning parameters would produce satisfactory outputs more efficiently and effectively. However, the noise block could be inserted back into the state space and the output will be similar for the same combination of tuning parameter values. The one adjustment that might need to be made could be to τ_f to correct for noise more appropriately.

4.8 Accuracy of Transfer Function Model Approximation

Now satisfied with the tuning parameters and output behaviour for the PID controller configured for the black box, the PID controller configured for the transfer function model was revisited to investigate whether the transfer function model would also produce an output within the performance specifications for the similar tuning parameters that yielded a satisfactory response from the black box. First, the correct combination of tuning parameters were substituted into the PID controller for the transfer function model without a parallel feedforward loop. As can be seen in the figures below, despite the transfer function model bode plot corroborating the black box bode plot, the PID controller configured for the transfer function model does not yield a satisfactory output.

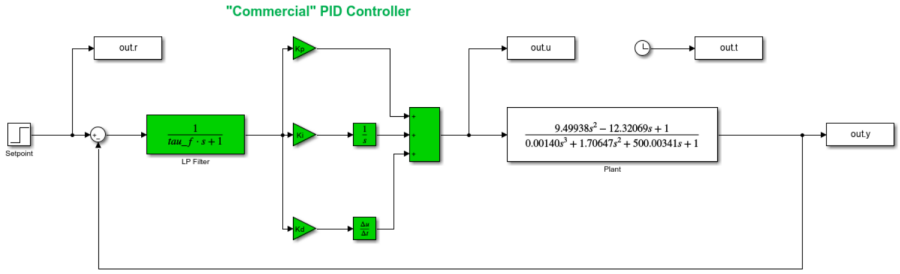

Figure 16: Output of PID controller for transfer function model provided stepped input, $K_p = 9.63$, $K_i = 0.0412164$, $K_d = 1.5$, $\tau_f = 10$

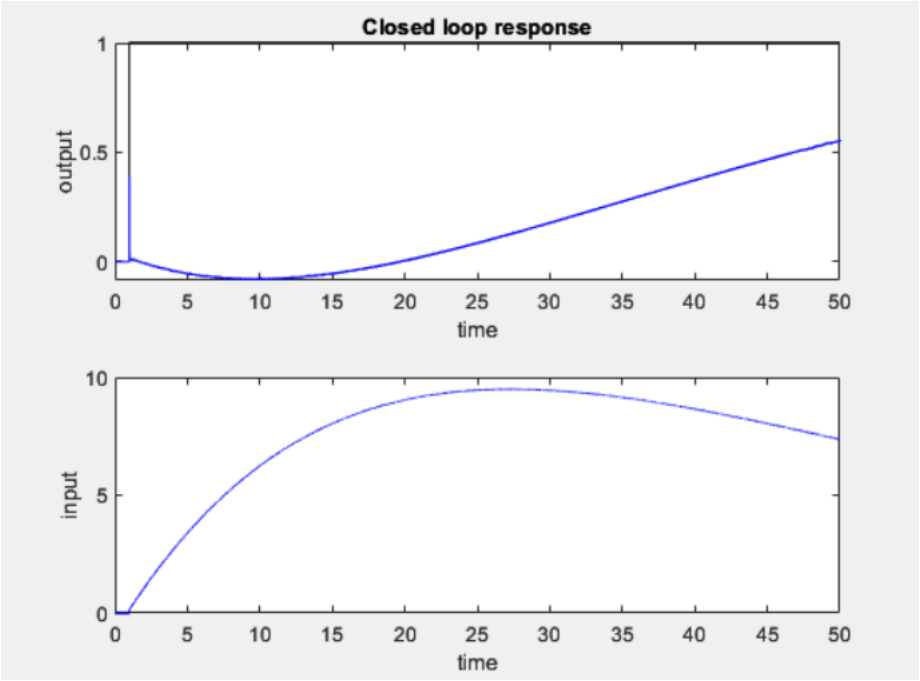

Figure 17: Close Loop Response of Controller

However, when the PID controller for the transfer function model was modified to include a parallel feedforward loop with the same design as the parallel feedforward loop used in the PID controller for the black box, almost a perfect response was produced.

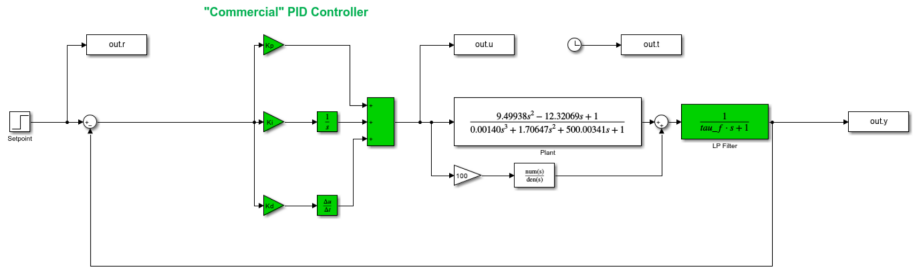

Figure 18: Output of PID controller for transfer function model provided stepped input, $K_p = 9.63$, $K_i = 0.0412164$, $K_d = 1.5$, $\tau_f = 10$, $L = 100$, with parallel feedforward loop

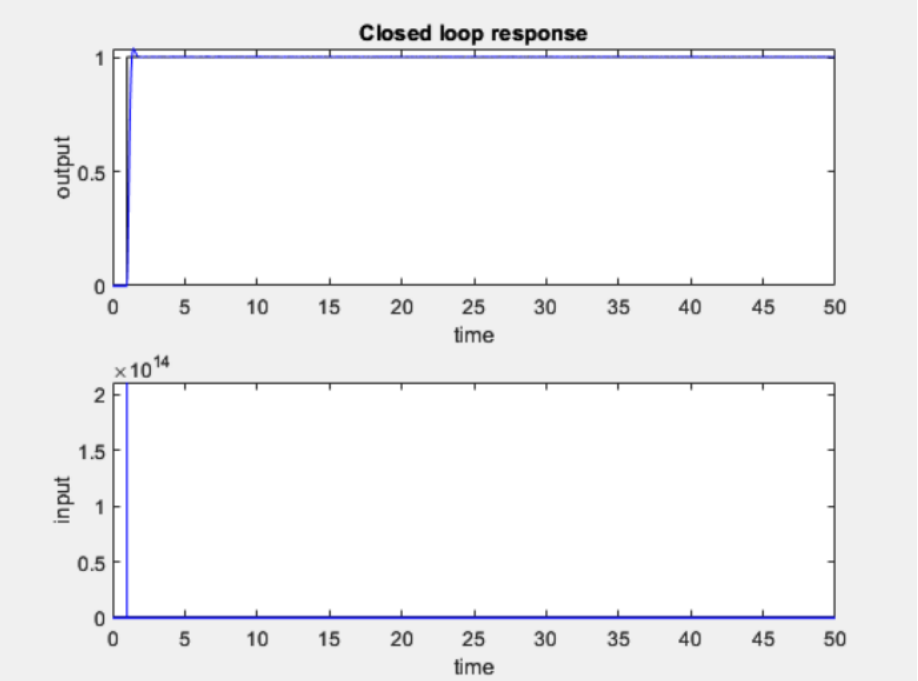

Figure 19: Output of above controller

These findings indicate there may exist discrepancies of some form between the derived transfer function model and the black box itself. However, they would also imply that once the non-minimum phase system of the transfer function model had also achieved minimum phase, for the same gain constant value, $L = 100$, that allowed the black box system to achieve minimum phase, a satisfactory output well within the performance specifications will be produced for the values $K_p = 9.63$, $K_i = 0.0412164$, $K_d = 1.5$ and $\tau_f = 10$ as used by the PID controllor for the black box.

5 Triple Bottom Line

When the team was selecting an application for the control system, Triple Bottom Line impact was one of the main considerations. When subjected to a Triple Bottom Line analysis, the chosen application of the brainwave frequency control system performed very well.

5.1 Societal Impact

The societal benefits of the implementation of the brainwave frequency control system are numerous. As mentioned previously, one in three people experience insomnia symptoms [9]. This means that one in three people could directly

benefit from this device by using it when they sleep. With improved sleep quality, they improve their memory, learning ability, and mental health [7] [8]. It is not only one third of the population that benefits from this device. While one third directly benefit from using this device, many people who are not in this one third indirectly benefit from its implementation. The benefits extend to the friends and family of the users, who will be happy to see an improvement in their friend or family member's quality of life.

5.2 Environmental Impact

While the implementation of the brainwave frequency control system benefits society more than it benefits the environment, the environmental benefit still exists. A study from Sleep Foundation shows that when people don't get enough sleep they tend to overeat [20]. As mentioned in the above paragraph, one in three people experience insomnia symptoms, so one third of the world may be eating more food than they need to because of poor sleep quality. By improving sleep quality with the usage of the brainwave frequency control system, a more regulated diet can be achieved. It's also important to note that 26% of all greenhouse gas emissions come from food production [21]. Therefore, with a large percentage of the population reducing unnecessary food consumption, greenhouse gas emissions will decrease.

5.3 Economic Impact

When evaluating profitability, the implementation of the brainwave frequency control system performed well. The estimated cost to produce a single unit is approximately $1000. This price comes from the average cost of an EEG (electroencephalogram) of $700 combined with the average cost of a tDCS device, which is $220. This sums to $920, and then after considering assembly costs of $80, the approximate total cost is $1000.

At this cost, the brainwave frequency control system was deemed to be profitable, as the user receives numerous benefits for the price of the device. This product can greatly improve the user's quality of life, as sleep quality affects memory, learning ability and mental health [7] [8]. The team feels that $1000 to greatly improve overall quality of life is a very worthy investment. However, not everyone can afford this, and that is also something that was taken into consideration. If, after its implementation, this device proves effective, deals may be made with the government to increase the accessibility of the device. Devices would be sold to the government, and doctors would prescribe the device to a willing and eligible patient and have the cost of the device covered by healthcare or health insurance.

References

[1] A. E. Tutorials, "Pv solar panel orientation and positioning," April 2018, [Accessed: 09-Mar-2023]. [Online]. Available: https://www.alternative-energy-tutorials.com/solar-power/solar-panel-orientation.html#:~:text=Solar/20PV/20modules/20and20panels,relies/20upon/20these/20two/20values.

[2] M. University, "Controlling fission," November 2020, [Accessed: 09-Mar-2023]. [Online]. Available: https://nuclear.mcmaster.ca/resources/how-does-it-work-2/controlling-fission/#:~:text=In/20contrast/2C/20in/20a/20nuclear,of/20the/20uranium/2D235/20fuel.

[3] "How to use excess power from solar panels," [Accessed: 09-Mar-2023]. [Online]. Available: https://photonbrothers.com/blog/how-use-excess-power-solar-panels/.

[4] "Selling energy back to the grid-how you can reap profit through ontario's fit program," March 2015, [Accessed: 09-Mar-2023]. [Online]. Available: https://www.insidehalton.com/shopping-story/5461551-selling-energy-back-to-the-grid-how-you-can-reap-profit-through-ontario-s-fit-program/.

[5] Wenli, "How much do solar inverters cost," April 2022, [Accessed: 09-Mar-2023]. [Online]. Available: https://luxpowertek.com/blog/solar-inverters-cost.

[6] F. P. Cappuccio, L. D'Elia, P. Strazzullo, and M. A. Miller, "Sleep duration and all-cause mortality: A systematic review and meta-analysis of prospective studies," May 2010, [Accessed: 09-Mar-2023]. [Online]. Available: https://www.ncbi.nlm.nih.gov/pmc/articles/PMC2864873/.

[7] "Sleep, learning, and memory," [Accessed: 10-Mar-2023]. [Online]. Available: https://healthysleep.med.harvard.edu/healthy/matters/benefits-of-sleep/learning-memory

[8] "Mental illness associated with poor sleep quality according to largest study of its kind," October 2021, [Accessed: 10-Mar-2023]. [Online]. Available: https://www.camh.ca/en/camh-news-and-stories/mental-illness-associated-with-poor-sleep-quality

[9] "Insomnia: What it is, causes, symptoms, and treatment," February 2023, [Accessed: 09-Apr-2023]. [Online]. Available: https://my.clevelandclinic.org/health/diseases/12119-insomnia.

[10] "Insomnia," October 2016, [Accessed: 07-Apr-2023]. [Online]. Available: https://www.mayoclinic.org/diseases-conditions/insomnia/diagnosis-treatment/drc-20355173.

[11] J. Summer, "Alpha waves and sleep," July 2022, [Accessed: 07-Mar-2023]. [Online]. Available: https://www.sleepfoundation.org/how-sleep-works/alpha-waves-and-sleep.

[12] H. R. Siebner, G. Hartwigsen, T. Kassuba, , and J. C. Rothwell, "How does transcranial magnetic stimulation modify neuronal activity in the brain? implications for studies of cognition," October 2009, [Accessed: 10-Mar-2023]. [Online]. Available: https://www.ncbi.nlm.nih.gov/pmc/articles/PMC2997692/.

[13] "What is transcranial direct current stimulation?" [Accessed: 06-Mar-2023]. [Online]. Available: https://neuromodec.org/what-is-transcranial-direct-current-stimulation-tdcs/.

[14] H. Thair, A. Holloway, R. Newport, and A.Smith, "Transcranial direct current stimulation (tdcs): A beginner's guide for design and implementation," November 2017, [Accessed: 07-Mar-2023]. [Online]. Available: https://www.frontiersin.org/articles/10.3389/fnins.2017.00641/full

[15] F. Fregni, M. A. Nitsche, C. K. Loo, P. M. A. R. Brunoni, J. Leite, S. Carvalho, N. Bolognini, W. Caumo, N. J. Paik, M. Simis, K. Ueda, H. Ekhitari, P. Luu, D. M. Tucker, W. J. Tyler, J. Brunelin, A. Datta, C. H. Juan, G. Venkatasubramanian, P. S. Boggio, and M. Bikson, "Regulatory considerations for the clinical and research use of transcranial direct current stimulation (tdcs): Review and recommendations from an expert panel," March 2015, [Accessed: 09-Mar-2023]. [Online]. Available: https://www.ncbi.nlm.nih.gov/pmc/articles/PMC4431691/.

[16] K. Stanton, "4 major class ii medical device requirements," May 2021, [Accessed: 07-Mar-2023]. [Online]. Available: https://www.qualio.com/blog/4-major-class-ii-medical-device-requirements/.

[17] A. Kuersten and R. Hamilton, "Minding the 'gaps' in the federal regulation of transcranial direct current stimulation devices," May 2016, [Accessed: 07-Mar-2023]. [Online]. Available: https://academic.oup.com/jlb/article/3/2/309/1751229.

[18] D. Pacheco, "Deep sleep: How much do you need?" March 2023, [Accessed: 07-Mar-2023]. [Online]. Available: https://www.sleepfoundation.org/stages-of-sleep/deep-sleep/.

[19] J. Bennett, A. Bhasin, J. Grant, and W. C. Lim, "Pid tuning via classical methods," May 2023, [Accessed: 07-Mar-2023]. [Online]. Available: https://eng.libretexts.org/Bookshelves/Industrial_and_Systems_Engineering/Chemical_Process_Dynamics_and_Controls_(Woolf)/09%3A_Proportional-Integral-Derivative_(PID)_Control/9.03%3A_PID_Tuning_via_Classical_Methods

[20] R. Newsom, "The connection between diet, exercise, and sleep," March 2023, [Accessed: 10-Mar-2023]. [Online]. Available: https://www.sleepfoundation.org/physical-health/diet-exercise-sleep.

[21] H. Ritchie and M. Roser, "Environmental impacts of food production," December 2022, [Accessed: 10-Mar-2023]. [Online]. Available: https://ourworldindata.org/environmental-impacts-of-food